Astronomy & Astrophysics manuscript no. 2DKoll-I
March 26, 2009

LETTER TO THE EDITOR

Protostellar collapse: rotation and disk formation

Werner M. Tscharnuter, Johannes Schönke, Hans-Peter Gail, and Ekaterina Lüttjohann

Zentrum für Astronomie (ZAH), Institut für Theoretische Astrophysik (ITA), University of Heidelberg, Albert-Überle-Str. 2, 69120 Heidelberg, Germany

Received / Accepted

ABSTRACT

We present some important conclusions from recent calculations pertaining to the collapse of rotating molecular cloud cores with axial symmetry, corresponding to evolution of young stellar objects through classes 0 and begin of class I. Three main issues have been addressed: (1) The typical timescale for building up a preplanetary disk – once more it turned out that it is of the order of one free-fall time which is decisively shorter than the widely assumed timescale related to the so-called "inside-out collapse"; (2) Redistribution of angular momentum and the accompanying dissipation of kinetic (rotational) energy – together these processes govern the mechanical and thermal evolution of the protostellar core to a large extent; (3) The origin of calcium-aluminium-rich inclusions (CAIs) – due to the specific pattern of the accretion flow, material that has undergone substantial chemical and mineralogical modifications in the hot ($\gtrsim 900$ K) interior of the protostellar core may have a good chance to be advectively transported outward into the cooler remote parts ($\gtrsim 4$ AU, say) of the growing disk and to survive there until it is incorporated into a meteoritic body.

Key words. Stars: formation – accretion – planetary systems: protoplanetary disks

1. Introduction

Stars are thought to form from regions within molecular clouds that for some reason became gravitationally unstable and started to collapse under the influence of their own gravitational attraction (see, e.g., Larson, 2003; McKee & Ostriker, 2007). It is clear that angular momentum (e.g., Bodenheimer, 1995; Tohline, 2002) and magnetic fields (e.g., Pudritz et al., 2008) play an important role during many stages of protostellar collapse. Angular momentum is particular important because it is responsible for the formation of accretion disks that are the birthplaces of planetary systems. Therefore, the study of rotating collapse is inevitable if one intends to understand the formation of the Solar System and other planetary systems.

The earliest such studies are a number of analytic approaches for rotating collapse without (Terebey et al., 1984) and with (Allen et al., 2003) magnetic fields and analytic studies of disk formation (see Cassen, 1994, and references therein) and simple models for build-up and evolution of accretion disks (e.g., Lin & Pringle, 1990; Nakamoto & Nakagawa, 1994). These suffer from that they introduce a number of approximations on the nature of the collapse process that appear plausible but lack justification.

In the past two decades various attempts have been made, therefore, to follow the 2-D and 3-D collapse of rotating protostellar fragments by means of extended numerical calculations (e.g., Boss, 1989; Bodenheimer et al., 1990; Yorke et al., 1993; Saigo et al., 2008, to give a few examples) based on grid-methods, by a solution method based on a series development into orthogonal polynomials (Tscharnuter, 1987), and by studies based on the SPH-method (e.g., Walch et al., 2009). However, because of lack of spatial resolution almost all of these studies followed only the first collapse phase up to the formation of the first core. Neither the second collapse of the core to stellar dimensions ($\lesssim 1\,\mathrm{R}_\odot$) could be followed, nor the formation of the inner part of the accretion disk on size scales $\ll 1$ AU. Only the model of Tscharnuter (1987) and the recent study of Saigo et al. (2008) achieved sufficient resolution to follow the second collapse, but Saigo et al. (2008) neglects most of the basic physics and considers only an over-simplified equation of state.

Many of the investigations mainly focus on the individual stability behaviour of the rapidly spinning, flattened, quasi-equilibrium "cores" that form in the innermost optically thick parts of collapse flows. It has long been known that, for a rotating self-gravitating equilibrium configuration, the ratio of rotational over gravitational energy, $\theta := E_\mathrm{rot}/\left|E_\mathrm{grav}\right|$,[1] is the appropriate parameter to indicate the onset of secular, for $\theta \simeq 0.14$, and dynamical, for $\theta \simeq 0.27$, instability. This is a standard result for *homogeneous* equilibria, but interestingly enough, in a series of papers Bodenheimer & Ostriker, 1970, 1973; Ostriker & Bodenheimer, 1973 were able to show that these two critical numbers still hold for more general rotating polytropes, almost independently of the polytropic index, n.

Due to this remarkable finding extensive 3-D calculations have been conducted in order to explore the fate of rapidly spinning "naked" protostellar cores by following the onset of the dynamical instability and its development into the nonlinear regime. Much effort has gone into clarifying the growth and saturation of the self-gravitating non-axisymmetric modes (bars, spirals, mixed forms) and their mutual interactions which drive a very effective redistribution of the cores' angular momentum (e. g., Pickett et al., 1996; Toman et al., 1998; Pickett et al., 1997; Imamura et al., 2000).

In this letter we present some results of a new model calculation that follows for the first time simultaneously the evolution of a rotating Bonnor-Ebert-sphere-like initial state with $\sim 1\,\mathrm{M}_\odot$

Send offprint requests to: W. M. Tscharnuter,
e-mail: wmt@ita.uni-heidelberg.de

[1] Usually written $\beta := T/|W|$, but we wish to avoid confusion with T, the temperature, and β, the scaling parameter of the turbulent viscosity.

Table 1. Starting parameters.

Quantity	Symbol	Value	Dimension
mass	M	1.037	$M_\odot$
angular momentum	L	$2.682{\cdot}10^{53}$	g cm^2 s^{-1}
radius	R	$1.200{\cdot}10^{17}$	cm
spin angul. veloc.	Ω	$3.160{\cdot}10^{-14}$	s^{-1}
centrifugal barrier	$R_{\rm cfb}$	$1.504{\cdot}10^{15}$	cm
mean density	$\bar{\rho}$	$2.850{\cdot}10^{-19}$	g cm^{-3}
mean free-fall time	$\bar{t}_{\rm ff} = \sqrt{\frac{3\pi}{32G\bar{\rho}}}$	$1.247{\cdot}10^{5}$	yr
central density	$\rho_{\rm c}$	$5.326{\cdot}10^{-18}$	g cm^{-3}
central free-fall time	$t_{\rm ff,c} = \sqrt{\frac{3\pi}{32G\rho_{\rm c}}}$	$2.885{\cdot}10^{4}$	yr
temperature	T	10	K
ratio rot./grav. energy	$\theta = \frac{E_{\rm rot}}{\lvert E_{\rm grav}\rvert}$	$2.437{\cdot}10^{-3}$	–

initial mass through axially-symmetric first and second collapse to nearly stellar central densities and the early build-up and evolution of the associated accretion disk. The maximum resolution achieved amounts to about 0.03 $R_\odot$ in the central parts. The adaptive grid is chosen in a way that the innermost rigidly rotating homogeneous sphere always contains a fraction of 10^{-6} of the total mass. The simulation covers the evolutionary phases of young stellar objects corresponding to class 0 and early class I. It clearly demonstrates the rapid co-formation of a compact stellar object and a very extended accretion disk within a period of no more than $\sim$ 1.1 free-fall times. The model includes all of the essential physics of the problem: hydrodynamics, gravity, radiative transfer (in Eddington approximation), and a realistic equation of state including effects of sublimation of ice and dust on the opacity.

By using a fully implicit numerical method (see Section 2) we are now able to follow the collapse of a slowly rotating, slightly Jeans-unstable molecular cloud fragment with axial symmetry.

2. Methods

The most frequently applied numerical methods – such as nested grids by Saigo et al. or SPH by Walch et al. – have in common that they are of explicit type ("forward" time differences), i. e., they are subjected to the Courant-Friedrichs-Lewy (CFL) condition for the timestep so as to warrant numerical stability. In fact, the CFL-timestep becomes prohibitively low with respect to the accretion time, if the structure of the hot stellar core is to be sufficiently well resolved. This is why explicit methods of any kind are genuinely unsuited for attacking the overall problem of stellar formation in a consistent way.

Unfortunately, appropriate implicit methods ("backward" time differences) have been worked out only for 1-D and 2-D collapse problems with spherical and axial symmetry, respectively (see, e. g., Wuchterl & Tscharnuter, 2003; Tscharnuter, 1987). Although implicit numerical schemes do not suffer from the CFL-condition, they demand, after all, the solution of a huge system of non-linear equations which is computationally expensive. Thus, implicit methods are useful only if the physical processes to be considered exhibit a hierarchy of timescales and the system as a whole evolves into a quasi-stationary state. If the longest timescale exceeds the smallest one by a large amount, the use of implicit methods is mandatory, as is in our case, where the accretion time is several orders of magnitude longer than the oscillation period of the stellar core.

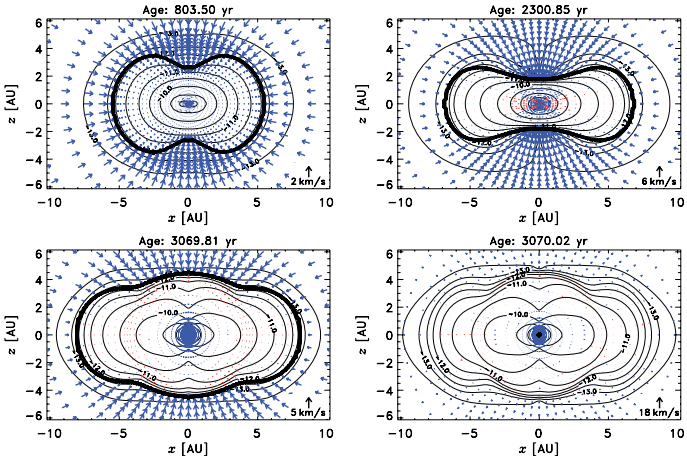

Fig. 1. Meridional cross sections. Displayed are equi-density contours, the spacing being 0.5 dex, and the velocity field. Red "spots" indicate expansion (cf. Fig. 3a). The closed heavy line marks the accretion shock, the arrow at the lower right corner of the four panels represents the respective maximum infall velocities. Upper row: snapshots slightly after B and before C, respectively. Lower row: snapshots for D and E (cf. Fig. 2). At E (right panel) two shocks, an outer and an inner one, bounding the growing "pre-planetary" disk and the "stellar" core, respectively, coexist (not displayed here, but cf. Fig. 4).

For a detailed description of the method which the implicit 2-D hydrodynamical code is based on we refer to Tscharnuter (1987). For the equation of state, dissociation of H_2 and ionisation of H and He is taken into account; the opacities at low temperatures are dominated by dust with and without ice mantles. In a spherical polar coordinate system, we discretize the variables on a staggered radial grid (256 gridpoints) and represent the dependence on the polar angle by choosing a Legendre expansion (up to 27 coefficients) for each primary variable. The discretized equations are written in conservation form on a self-adaptive radial grid according to Dorfi & Drury (1987), shock fronts are smoothed out by artificial (tensor-) viscosity.

Concerning the coefficient of turbulent viscosity, $\nu_{\rm tur}$, we have adopted the so-called β-viscosity prescription of Duschl et al. (2000), an extension of the well-known, but likewise heuristic, α-viscosity for application to self-gravitating disks. To be specific, $\nu_{\rm tur} := \beta r^2\Omega$, with r being the radial coordinate, Ω the (local) angular velocity, and $\beta = 10^{-4}\ldots10^{-2}$ the inverse of the critical Reynolds number indicating the onset of turbulence. In our calculation we have chosen $\beta = 10^{-2}$.

3. Results and conclusions

3.1. Initial configuration and the first collapse phase

Table 1 lists a set of appropriate starting parameters leading to the collapse of a rotating protostellar cloud fragment. The (optically thin) Bonnor-Ebert-sphere-like initial configuration exhibits already a moderate density concentration toward the centre and is assumed to rotate like a rigid body. The revolution period, $2\pi/\Omega = 6.3\cdot10^6$ yr, adopted in our calculation is large compared to the mean free-fall time. Hence, the centrifugal barrier is situated at a distance from the centre of only about 1 % of the cloud radius, and the collapse flow develops almost perfectly with spherical symmetry for most parts of the cloud.

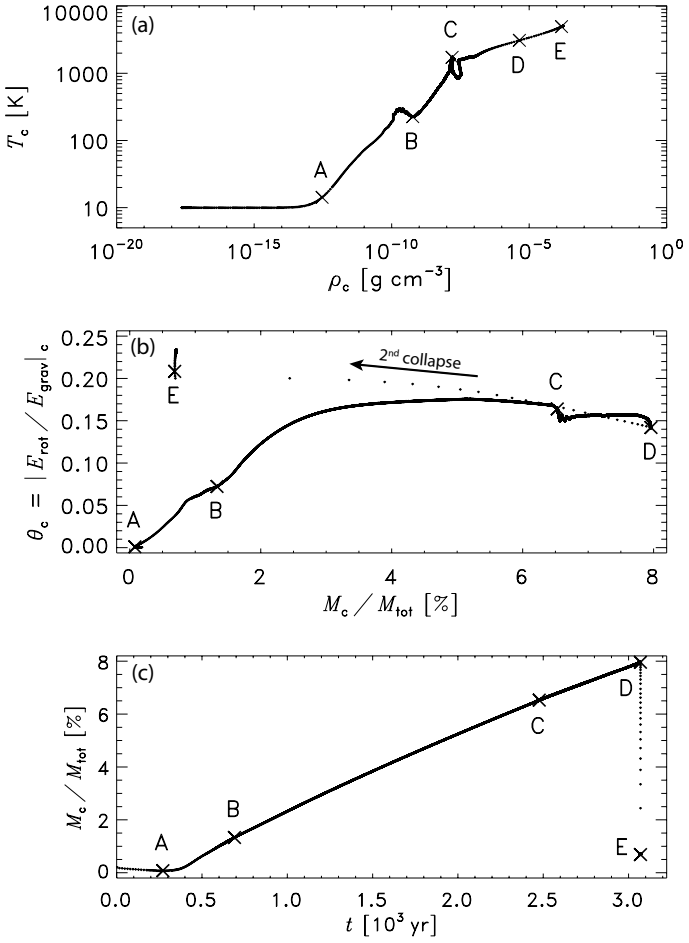

Fig. 2. Evolution of the core. (a): central density vs. central temperature. (b) ratio of rotational over gravitational energy vs. core mass. (c) core mass vs. time. For the meaning of labels A through E see Section 3.2.

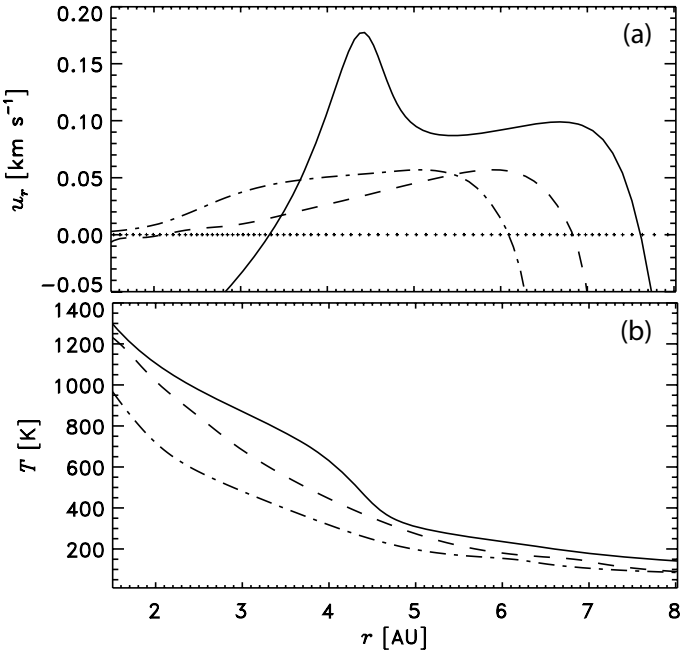

Fig. 3. Evolution of the core from its quasi-stationary stage to the end of the second collapse. Spatial distribution of (a) the radial velocity component, u_r, (b) the temperature, T, in the equatorial plane for three instants of time indicated by dash-dotted (2301 yr), dashed (2948 yr), and solid lines (3070 yr), respectively; crosses mark the gridpoints.

After about one mean free-fall time the temperature rises in the centre of the fragment and a quasi-hydrostatic core is going to form. It is thus convenient to reset the clock to zero when the optical depth of the collapsing fragment, counted from the outer edge to the centre, exceeds 2/3 for the first time (e. g., Wuchterl & Tscharnuter, 2003). This event may be attributed to the beginning of the protostellar evolution proper. All ages subsequently given are relative to this instant.

Shortly after age zero an accretion shock forms, that marks the natural boundary of a "core", a flattened quasi-hydrostatic rotating structure that is pressure-supported parallel and, in essence, centrifugally-supported perpendicular to the axis of rotation.

As the "core" we shall refer to the innermost *subsonic* region of the collapsing fragment, regardless of whether or not the accretion shock is present. During the main accretion phase the flow becomes indeed highly supersonic and a strong shock is present at any polar angle (cf. Fig. 1). However, the retarding effect of the centrifugal forces significantly reduces the velocity components perpendicular to the axis of rotation. Particularly close to the equatorial plane, this effect will sooner or later in the evolution weaken the local shock strength considerably or even make the flow discontinuity disappear completely. This will happen within only a few initial mean free-fall times. Then infall of matter from the envelope is eventually going to cease, whereas the "core" gradually turns into a veritable protoplanetary accretion disk.

The current simulations do not only cover the collapse proper, but also the formation and the beginning of the ensuing accretion phase of the disk-like core.

3.2. Formation and growth of the disk-like core

Figure 2 shows (a) the density-temperature-diagram for the very centre of the collapsing cloud, (b) the stability parameter θ_c as a function of the relative core mass M_c/M_{tot}, (c) the time dependence of the relative core mass. The labels A through E mark characteristic stages of the evolution:

A: The core starts to grow in mass;
B: continuation of the accretion after thermal relaxation caused by opacity effects (sublimation of ice mantels);
C: sublimation of the dust grains commences off-centre near the axis of rotation as a "hot polar cap", leaving a growing opacity gap and violent thermal relaxation effects;
D: start of the second collapse due to dissociation of H_2;
E: formation of the "stellar" core.

As the first important result, we have found a typical rise time, $M_c/\dot{M}_c$, of the core's mass to be only a small fraction (1–2 %) of the mean free-fall time, i. e., only a few thousand years. Figure 2c shows an almost constant accretion rate of $3\cdot10^{-5}\,M_\odot\,yr^{-1}$ lasting for about 2 600 yr, from slightly after "A" until "D" where the second collapse sets in. The dots between "D" and "E" represent the individual models tracing the dynamical transition (the "second collapse") from the disk-forming first core to the second "stellar" core.

Figure 1 demonstrates the increasing geometrical dimensions and the changing shape of the first core, which occurs

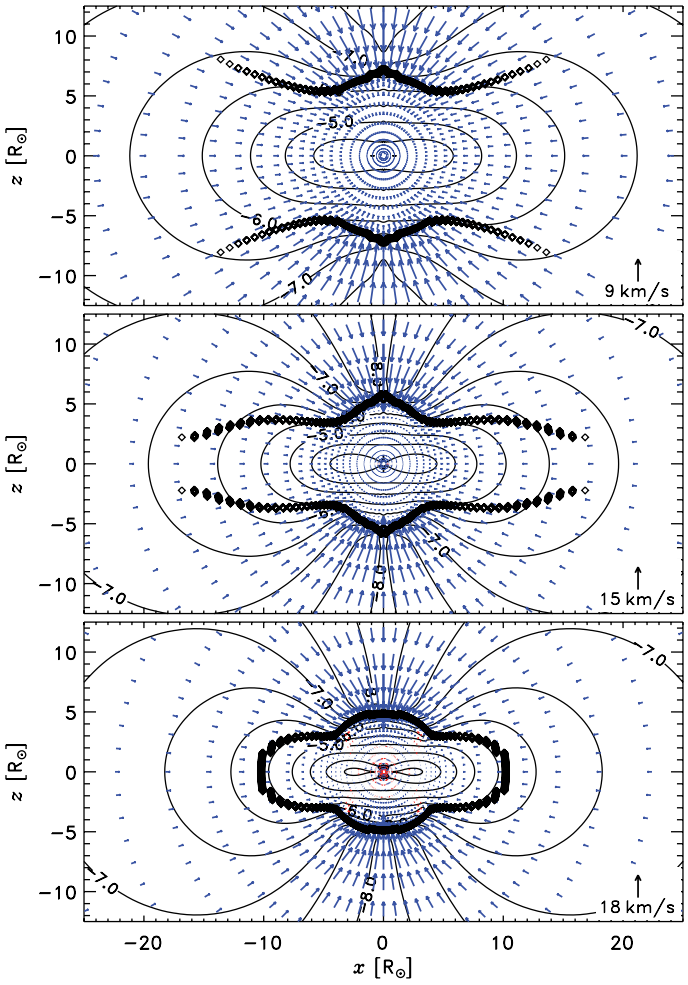

Fig. 4. Meridional cross sections (cf. Fig. 1). Formation of the "stellar" core on a very short timescale. Plotted are three snapshots of the final shock evolution at (from above) $t_0 - 10\,\mathrm{d}$, t_0, and $t_0 + 7\,\mathrm{d}$, respectively, with $t_0 = 3070\,\mathrm{yr}$. Note that now the geometrical dimensions are only several solar radii ($\mathrm{R}_\odot$).

within a few thousand years; the bulge in the polar direction, indicated by the route of the accretion shock in the vicinity of the rotational axis, is the result of a rather intricate interplay between redistribution of angular momentum, the accompanying generation of entropy (viz. heat), and transport of energy. The net effect are rising temperatures and lower rotation rates in the inner parts of the core, which is necessary to trigger the second collapse. As a matter of fact, test calculations have shown that without a certain amount of angular momentum transport the core would stay too cool and, hence, become prone to the onset of destructive gravitational instabilities that trigger binary formation.

A glimpse to Fig. 2b reveals that the first core cannot escape from running into the regime of secular instability. The ratio, $\theta = E_\mathrm{rot}/|E_\mathrm{grav}|$, quickly rises above the critical number of 0.14, so that already a small amount of dissipation will lead to symmetry breaking: The originally axisymmetric core will take on a triaxial shape and presumably evolve into a distinctive bar/spiral configuration exerting gravitational torques which, in turn, results in an enhanced redistribution of angular momentum. This finding may serve as motivation for our rather efficient turbulent (β-)viscosity with $\beta = 0.01$.

3.3. Formation of the "stellar" core

The second collapse is a result of the interplay between thermodynamics, redistribution of angular momentum as a dissipative process, and energy transport. Their combined effect is illustrated by Fig. 1: particularly in the central parts, angular momentum transport tends to defuse extrem flattening, while the heat input by the accompanying dissipation of rotational energy creates increasing pressure forces. As a consequence, the pressure distribution is becoming more spherical, and after some "incubation" period of slow contraction (between "C" and "D" in Fig. 2) dissociation of H_2 eventually leads to dynamical collapse ("D"–"E"). Figure 2b shows that the stability parameter, θ_c, approaches the critical number of 0.27 indicating dynamical instability. Interestingly enough, our axisymmetric model suggests the formation of a self-gravitating doughnut-like structure of the density distribution (cf. Fig. 4).

3.4. An intermediate hot solar nebula?

The model provides for the first time the initial temperature and density structure of the accretion disk and the flow pattern in the disk and its surroundings, including the accretion shocks, on scales down to much less than 1 AU. Figure 3b shows a rather hot inner disk region extending out to about 4 AU. This structure is not seen in earlier calculations because of lack of resolution; it lasts for a couple of 1 000 yr. This inner portion is hot enough for formation of materials like those found as calcium-aluminium rich inclusions (CAIs) in meteorites; it might be the "hot solar nebula" that cosmochemists always advocated for.

From the onset of disk formation on there is both accretion and a large-scale transport of matter (with velocities 10–$50\,\mathrm{m\,s^{-1}}$) close to the disk's midplane from the hot part outward to distances of several AU from the centre (cf. Figs. 1 and 3a). Material from the hot region may be mixed across the inner ~ 5 AU and part of this material may survive till the onset of planetesimal formation, since outflow close to the midplane continues to exist in later phases, though with reduced velocity (e.g., Keller & Gail, 2004). The model therefore seems to offer an explanation how the short, maybe as short as 20 000 yr (Jacobsen et al., 2008), CAI-forming period in the Solar Nebula is related to the earliest evolutionary phase of the accretion disk. If true, CAI formation follows immediately the second collapse and is a valid indicator for the formation time of the protoplanetary disk.

Acknowledgements. This work has been supported by the Forschergruppe 759, "The Formation of Planets: The Critical First Growth Phase" of the Deutsche Forschungsgemeinschaft (DFG).

References

Allen, A., Li, Z.-Y., & Shu, F. H. 2003, ApJ, 599, 363
Bodenheimer, P. 1995, ARA&A, 33, 199
Bodenheimer, P. & Ostriker, J. P. 1970, ApJ, 161, 1101
Bodenheimer, P. & Ostriker, J. P. 1973, ApJ, 180, 159
Bodenheimer, P., Yorke, H. W., Różyczka, M., & etal. 1990, ApJ, 355, 651
Boss, A. P. 1989, ApJ, 345, 554
Cassen, P. 1994, Icarus, 112, 405
Dorfi, E. A. & Drury, L. O. 1987, J. Comp. Phys., 69, 175
Duschl, W. J., Strittmatter, P. A., & Biermann, P. L. 2000, A&A, 357, 1123
Imamura, J. N., Durisen, R. H., & Pickett, B. K. 2000, ApJ, 528, 946
Jacobsen, B., Yin, Q., Moynier, F., et al. 2008, Earth Plan. Sci. Lett. 272, 353
Keller, C. & Gail, H.-P. 2004, A&A, 415, 1177
Larson, R. B. 2003, Reports on Progress in Physics, 66, 1651
Lin, D. N. C. & Pringle, J. E. 1990, ApJ, 358, 515
McKee, C. F. & Ostriker, E. C. 2007, ARA&A, 45, 565
Nakamoto, T. & Nakagawa, Y. 1994, ApJ, 421, 640

Ostriker, J. P. & Bodenheimer, P. 1973, ApJ, 180, 171
Pickett, B. K., Durisen, R. H., & Davis, G. A. 1996, ApJ, 458, 714
Pickett, B. K., Durisen, R. H., & Link, R. 1997, Icarus, 126, 243
Pudritz, R. E., Banerjee, R., & Ouyed, R. 2008, ArXiv e-prints
Saigo, K., Tomisaka, K., & Matsumoto, T. 2008, ApJ, 674, 997
Terebey, S., Shu, F. H., & Cassen, P. 1984, ApJ, 286, 529
Tohline, J. E. 2002, ARA&A, 40, 349
Toman, J., Imamura, J. N., & Pickett, B. K. 1998, ApJ, 497, 370
Tscharnuter, W. M. 1987, A&A, 188
Walch, S., Burkert, A., Naab, T., & Gritschneder, M. 2009, ArXiv e-prints
Wuchterl, G. & Tscharnuter, W. M. 2003, A&A, 398, 1081
Yorke, H. W., Bodenheimer, P., & Laughlin, G. 1993, ApJ, 411, 274